A Low-Threshold Nonlinear-Amplifying-Loop-Mirror Mode-Locked Bismuth-Doped Fiber Laser Using A 3×3 Coupler

Kuen Yao Lau, Jinwen Lin, Sergei Firstov, Fedor Afanasiev, Xiaofeng Liu, and Jianrong Qiu

***Abstract*—Passive mode-locking plays a crucial role in generating ultrafast laser pulses and high-quality beams. However, traditional figure-of-eight laser cavities often require additional intra-cavity amplitude modulators, tapping or a two-gain-segment design to initiate mode-locking, leading to increased complexity and loss within the cavity. Here we propose a novel approach utilizing a 3×3 optical coupler to address these challenges. This work was performed at the novel communication O-band using bismuth-doped phosphosilicate glass fiber, where most rare-earth-doped silica fibers are inaccessible. By integrating a bismuth-doped nonlinear-amplifying-loop-mirror with a 3×3 optical coupler operating at 1310 nm, we achieve stable mode-locking at a significantly reduced pump power of 119.9 mW. Notably, the incorporation of a 120-degree (2π/3) phase difference results in an initiation threshold reduction of at least by 45% for NALM laser cavity using a symmetrical 2×2 optical coupler, lower pump power that maintain stable mode-locking by 26% compared to using an asymmetrical 2×2 optical coupler (70:30), and at least a twofold increase in output power of up to 6.839 mW. These findings underscore the potential of our optimized structure for improving performances of fiber lasers operating at the optical communication O-band.**

***Index Terms*—Bismuth-doped fibers, fiber lasers, mode-locking, nonlinear-amplifying-loop-mirror, optical coupler.**

Manuscript received 19 March 2024; revised 25 June 2024 and 4 August 2024; accepted 10 August 2024. Date of publication 16 August 2024; date of current version 2 January 2025. This work was supported in part by the National Key R&D Program of China under Grant 2021YFB2802000, in part by the National Natural Science Foundation of China under Grant U20A20211, in part by the National Natural Science Foundation of China under Grant 62175210, Grant 62005240, and Grant W2433154, and in part by the Natural Science Foundation of Zhejiang Province under Grant LY21F050005 and Grant LR21E020005. *(Kuen Yao Lau and Jinwen Lin contributed equally to this work.) (Corresponding authors: Kuen Yao Lau; Jianrong Qiu.)*

Kuen Yao Lau is with the School of Optoelectronic Science and Engineering & Collaborative Innovation Center of Suzhou Nano Science and Technology, Soochow University, Suzhou 215006, China (e-mail: laukuenyao@suda.edu.cn).

Jinwen Lin and Jianrong Qiu are with the College of Optical Science and Engineering and State Key Lab of Modern Optical Instrumentation, Zhejiang University, Hangzhou 310027, China (e-mail: 3220101949@zju.edu.cn; qjr@zju.edu.cn).

Sergei Firstov is with the Prokhorov General Physics Institute of the Russian Academy of Sciences, Dianov Fiber Optics Research Center, 119333 Moscow, Russia (e-mail: fir@fo.gpi.ru).

Fedor Afanasiev is with the G.G. Devyatyh Institute of Chemistry of High Purity Substances of the Russian Academy of Sciences, 603951 Nizhny Novgorod, Russia (e-mail: kamerton-fis@mail.ru).

Xiaofeng Liu is with the School of Materials Science and Engineering, Zhejiang University, Hangzhou 310027, China (e-mail: xfliu@zju.edu.cn).

This article has supplementary material provided by the authors and color versions of one or more figures available at https://doi.org/10.1109/JLT.2024.3445155.

Digital Object Identifier 10.1109/JLT.2024.3445155

I. Introduction

MODE-LOCKED fiber lasers have found wide applications in optical frequency metrology [1], [2], nonlinear optics [3], micromachining [4], [5], [6], medicine [7], and telecommunication [8], [9], to name a few. The importance of these lasers derives from their compact size, robust beam quality, and lightweight construction. Active mode-locking, a technique for achieving phase locking among longitudinal modes within the cavity through periodic modulation of external signals, offers benefits such as symmetrical pulse shape, tunable central wavelength, and the capacity for high-order mode-locking [10], [11], [12], [13]. However, limited by the modulation pulse width, the output pulse width is typically constrained to the picosecond level. Furthermore, the incorporation of a modulation device introduces additional loss within the cavity, posing challenges for realizing an all-fiber configuration. To generate sub-picosecond and femtosecond pulses and to mitigate the complexity of ultrashort pulse locking by exploiting the nonlinear effect of lasers, passive mode-locking has been proposed [14], which operates by utilizing the nonlinear absorption characteristics of saturable absorbers (SAs) [15]. Material-based SAs leverage the saturable absorption features of materials such as semiconductor SA mirrors (SESAMs) [16], carbon nanotubes (CNTs) [17], [18], and graphene [19], [20]. SESAMs perform the capability of self-starting continuous mode-locking and good control over SA parameters. However, the narrow tuning wavelength range, complex fabrication, and low damage threshold of SESAM still need to be addressed. CNTs and graphene, positioned as a simpler and lower-cost alternative, which, however, continued to face challenges of degradation, low damage threshold and poor tunability [21].

On the contrary, artificial saturable absorbers (ASAs), including nonlinear polarization rotation (NPR) [22], nonlinear optical loop mirror (NOLM) [23], and nonlinear amplifying loop mirror (NALM) [24], [25], offer benefits of ultrafast recovery time, environmental stability, and minimal degradation over time [26]. NPR utilizes nonlinear optical effects dependent on the intensity of input pulses to manipulate the polarization state, generating ultrashort pulses via a polarization controller. Nevertheless, NPR has the drawbacks of being sensitive to environmental perturbations, which causes fluctuations in polarization state and unstable mode-locking. Therefore, NALM in the figure-of-eight (Fo8) laser cavity is designed to ensure robust performance. The

phase shift of counter-propagating beams undergoes asymmetric changes, culminating in coherent interference and stable pulse generation [27].

Reducing the threshold of self-starting mode-locking in the Fo8 NALM is an unresolved problem. Zhou et al. [28] have proposed a two-pump structure in a Fo8 laser cavity to initiate mode-locking. Alternative approaches involve incorporating additional components such as amplitude/phase modulation or tapping mechanisms [29]. However, for the two-pump structure, the combination of two SAs or additional components results in a complex structure and a decrease in repetition rate. Therefore, there is a demand for a simpler mode-locking initiation method characterized by a low threshold of self-starting, additional nonlinear phase difference, reduced laser cavity length, and simplified configuration. Notably, a theoretical model based on a 3×3 transfer matrix has been proposed to elucidate the properties of the 3×3 optical coupler (OC), revealing that the transfer properties of the 3×3 OC can be characterized when the splitting ratio data is available [30], [31], [32], [33], [34]. Consequently, a symmetric 3×3 OC can generate a 120-degree ($2\pi/3$) phase difference, whereas a 2×2 OC with a splitting ratio of 50:50 can only provide a 90-degree ($\pi/2$) phase difference [35]. A NOLM utilizing symmetric 2×2 OC acts as an optical reflective mirror, which requires an attenuator to interpose asymmetrical loss [36], such as via a nonlinear absorbing loop mirror [37], bending fiber to induce attenuation-imbalanced NOLM [38], using a variable optical attenuator [39] and using an additional OC in the loop [40]. This results in the transmissivity relies on both transmission of the attenuator and position of the attenuator in the loop, thus leading to the need of higher pump power threshold to generate mode-locking and might requires the use of single-mode fiber of more than 50 meters in the laser cavity or using a highly nonlinear fiber [38], [40]. On the other hand, a symmetric 3×3 OC has a power splitting ratio of ∼33/33/33, which induces a phase shift of $2\pi/3$ for any three ports of the OC. This denotes that the transmission curve of a symmetric 3×3 OC is shifted in phase by $2\pi/3$. In comparison to loss-induced NOLM utilizing a symmetric 2×2 OC, a non-vanishing relative transmission to output port is obtained for nonlinear phase difference at 0 rad using a symmetric 3×3 OC, thus enabling pulse build-up from noise and leads to a reduced pump power required for the self-starting of mode-locked laser operation [31], [32], [33], [34].

For O-band (∼1260 nm to ∼1360 nm) fiber lasers, lanthanide ions doped silica-based gain fibers do not exhibit high-quality emission, due to strong water absorption, low damage threshold, and low efficiency [41]. In comparison, bismuth-doped phosphosilicate glass fibers exhibit strong emission at O-band with a large bandwidth [42], [43], [44], [45]. Therefore, bismuth-doped fiber laser operating at 1310 nm, could pave the way for optical communications within the second telecommunication window.

In this work, we present a novel communication O-band mode-locked fiber laser using bismuth-doped phosposilicate glass fiber, where most rare-earth-doped silica fibers are inaccessible. Further, we demonstrate a mode-locked bismuth-doped fiber laser based on a 3×3 OC at 1310 nm. By using the 3×3 OC, we show that the pump power threshold is reduced to 299.6 mW. In addition, we demonstrate the initiation of mode-locking in the Fo8 laser cavity, which cannot be observed by a symmetrical 2×2 OC even at the highest pump power of 561 mW. Our results highlight the mode-locking initiation capability is improved by at least 45%. In addition, a lower pump power to maintain stable mode-locking by 26% is obtained by the 3×3 OC NALM laser cavity in comparison to an asymmetrical 2×2 OC NALM laser cavity with splitting ratio of 70:30. Furthermore, the output power generated by the 3×3 NALM is higher by at least 2 times than that achieved in the conventional 2×2 NALM Fo8 laser cavity.

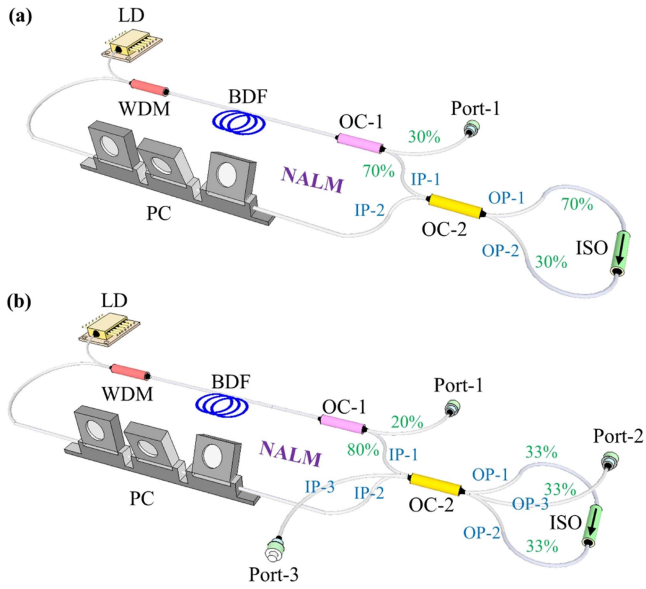

Fig. 1. Schematic diagram of NALM laser cavity using (a) 2×2 OC and (b) 3×3 OC.

II. Experimental Setup

The bismuth-doped fiber preform was fabricated by the modified chemical vapour deposition method utilizing an all-gas-phase deposition technology. This fiber preform was drawn into single-mode fibers using standard fiber drawing technique. The similar technical process was described in detail in earlier works [42], [43]. The main characteristics of the bismuth-doped fiber can be found in [43]. The laser cavity configurations based on a 2×2 OC and a 3×3 OC in our experiment is schematically shown in Fig. 1. In Fig. 1(a), the Fo8 laser cavity comprises a NALM and a mirror loop interconnected via a 2×2 OC with a splitting ratio of 50:50 for preliminary test. Laser signals propagate in opposite directions within the NALM configuration, including sufficient nonlinear phase shift. A section of ∼40 meters of single-mode bismuth-doped fibers (BDF) is utilized to provide asymmetrical loop configuration and sufficient gain to achieve stimulated emission laser under a pump power of ∼299.6 mW. In the NALM, a semiconductor laser diode (LD) and 1240/1310 nm wavelength division multiplexer (WDM) are employed to pump the BDF. A polarization controller (PC) is used to tune the polarization state of the counter-propagating beams. The NALM and mirror loop are integrated with the 2×2 OC, which allows coherent interference of the counter-propagating laser

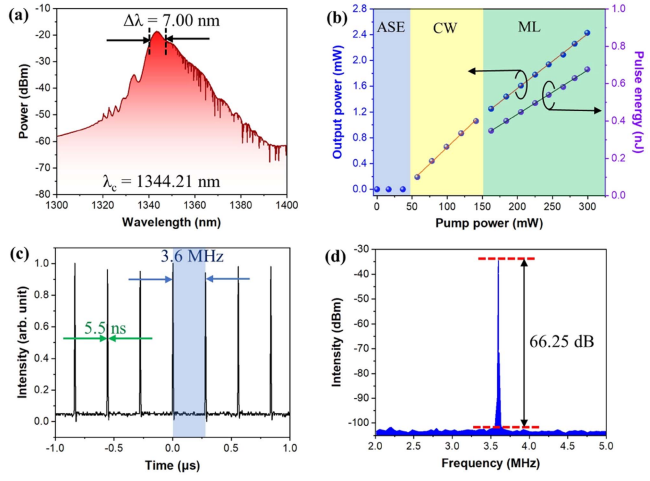

Fig. 2. Laser output measured from Port-1 for the NALM laser cavity using 2×2 OC. (a) Optical spectrum, (b) Power development curve, (c) Pulse train and (d) RF spectrum.

signals at input-1 (IP-1) and input-2 (IP-2); and the mirror loop is connected via two output ports (OP-1 and OP-2). The 2×2 OC has a splitting ratio of 70:30 and an additional tapping is provided for the initiation of mode-locking laser operation. In the mirror loop, an isolator (ISO) is adopted to ensure the unidirectional propagating of the laser signal. The 3×3 OC NALM fiber laser cavity is depicted in Fig 1(b). The primary distinction between the two configurations is that we adopt a symmetric 3×3 OC with coupling ratio of ∼33:33:33 to replace the 2×2 OC. Consequently, two additional ports: port-3 IP-3 and port-2 OP-3 are obtained. To maintain consistency and facilitate a fair comparison between 2×2 and 3×3 OC, a tap coupler with a splitting rate of 30:70 and 20:80 is added both in the 2×2 OC and 3×3 OC NALM, respectively.

III. Result and Discussion

We first measure the laser performance of a NALM using a symmetrical 2×2 OC with splitting ratio of 50:50. At pump power of 299.6 mW, a continuous-wave fiber laser output is observed at the center wavelength (λ_c) of ∼1326.75 nm with a 3-dB spectral bandwidth ($\Delta\lambda$) of ∼0.03 nm and output power of ∼3.157 mW, as illustrated in the Supporting Information, Fig. S1. The pump power is increased to a maximum value of ∼561 mW, which is below the initiation threshold for mode-locking operation. Therefore, the incorporation of asymmetrical 2×2 OC or the use of a symmetrical 3×3 OC is a viable choice to reduce the pump power threshold to initiate mode-locking operation of the NALM laser cavity. By implementing the experimental setup in Fig. 1, we compare the laser performance of the 2×2 OC NALM and the 3×3 OC NALM. Fig. 2(a) presents the optical spectrum measured from 2×2 OC NALM at the pump power of 299.6 mW. The λ_c and $\Delta\lambda$ of the mode-locked laser are measured to be 1344.21 nm and 7.00 nm, respectively. Stable mode-locked laser is maintained by reducing the pump power to 162.6 mW. In Fig. 2(b), the amplified spontaneous emission (ASE) region is observed below pump power of 36.94 mW.

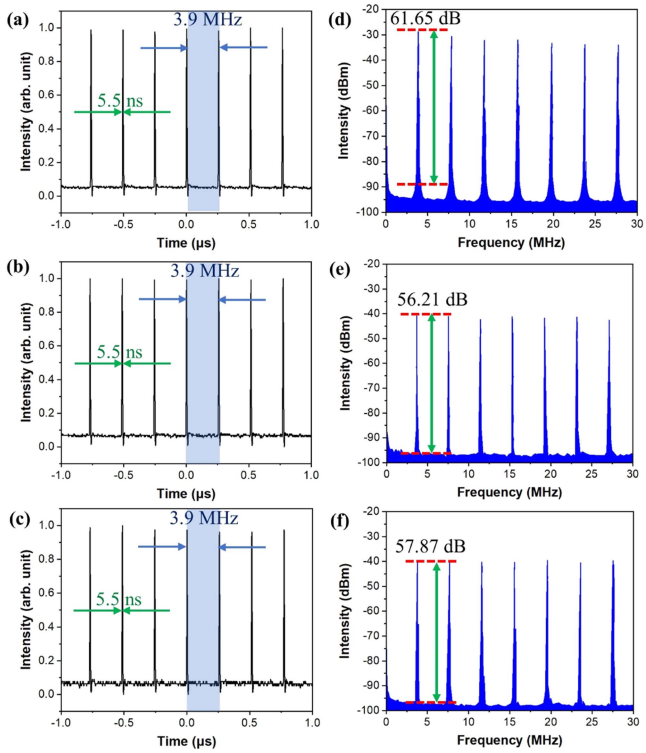

Fig. 3. Pulse trains and RF spectra for NALM laser cavity using 3×3 OC for (a,d) Port-1, (b,e) Port-2 and (c,f) Port-3.

The continuous-wave (CW) laser is attained at a pump power threshold of 36.94 mW, which is maintained until 141.1 mW. The output power of the CW laser region is recorded from 0.19 to 1.06 mW with a laser slope efficiency of 0.84%. In the mode-locking (ML) region, the output power is measured from 1.25 to 2.43 mW with a laser slope efficiency of 0.86%. The pulse energy is calculated by dividing output power of the ML laser to the pulse repetition rate, which is measured to be 3.6 MHz in Fig. 2(c). Therefore, the pulse energy is deduced to be between 0.35 to 0.68 nJ in the ML laser region (see Fig. 2(b)). Fig. 2(d) shows the radio frequency (RF) spectrum of the ML laser and the signal-to-noise ratio (SNR) is measured to be 66.25 dB.

Fig. 3(a)–(c) illustrate the pulse trains of the 3×3 NALM laser cavity, measured by the oscilloscope at the pump power of 299.6 mW. The pulse repetition rate of Port-1, 2, and 3 is remained at ∼3.9 MHz. The repetition rate is constant when the pump power is increased from 119.9 mW to 299.6 mW, corresponding to ∼55 meters of cavity length that includes ∼40 meters of BDF and single-mode fibers of other optical components. Moreover, the smooth peak of the pulse trains and the stable mode-locking operation are confirmed as illustrated in the Supporting Information, Fig. S2(a)–(f).

Fig. 3(d)–(f) present the RF spectrum of the 3×3 NALM laser cavity measured at a frequency span from 0 to 30 MHz, with the resolution bandwidth of 10 kHz and video bandwidth of 300 Hz. Across all the three ports, the SNR of ∼61.65, ∼56.21 and ∼57.87 dB is measured for Port-1, Port-2 and Port-3, respectively. A higher ground noise level of Port-1 is shown in Fig. 3(d), demonstrating that Port-2 and Port-3 showcase

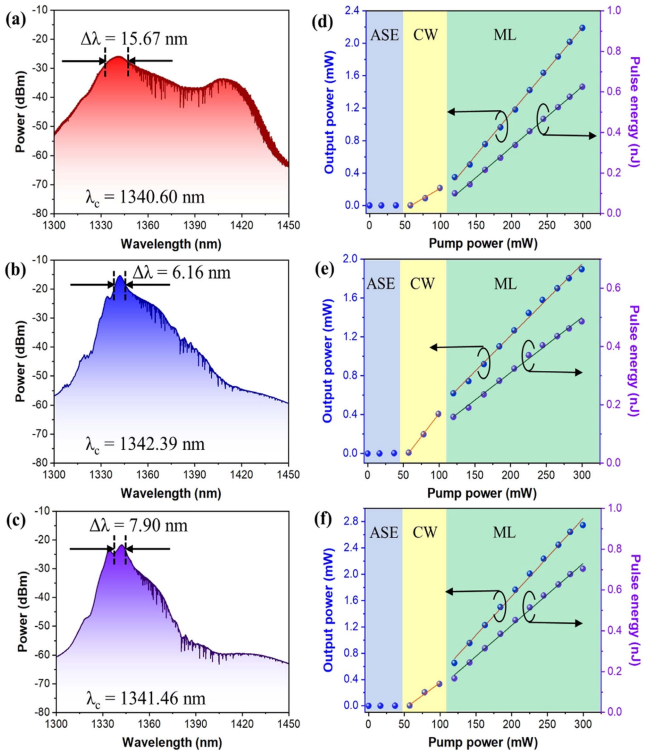

Fig. 4. Optical spectra and power development curves for NALM laser cavity using 3×3 OC for (a,d) Port-1, (b,e) Port-2 and (c,f) Port-3.

better performance of noise suppression. In particular, Port-1 is measured via the OC-1, which is placed after the bismuth-doped gain fiber, where this position has strong amplified spontaneous emission (ASE) signal due to the pumped gain fiber. Therefore, the measured optical spectrum in Fig. 4(a) has a high ASE signal measured together with the mode-locked laser, thus leading to high background noise in Fig. 3(d). Next, the loop mirror acts like a filter apparently, which suppress the ASE after the laser signal propagates through the OC-2, e.g., IP-3 (Port 2) and OP-3 (Port 3). This contributes to the suppression of the background noise in Fig. 3(e) and (f). Moreover, all RF spectra show the absence of modulation peaks. The absence of modulation peaks at the repetition rate of ∼3.9 MHz for the mode-locked lasers is presented with a clean single peak of the RF spectra, as illustrated in the Supporting Information, Fig. S3(a) and (b). In Fig. S3(c), there is a small side peaks at ∼4.4 MHz that might be due to intensity or phase fluctuation, or the inter-pulse beating of a multi-pulse laser output.

Fig. 4(a)–(c) show the optical spectra of the 3×3 NALM laser cavity. The center wavelengths of all ports remain stable at ∼1340 nm, whereas the widest spectral bandwidths (Δλ) at full-width of half maximum (FWHM) are attained from Port-1 of 15.67 nm, followed by Port-3 (7.90 nm) and Port-2 (6.16 nm). Owing to the lack of an autocorrelation device, the FWHM transform-limited pulse duration is calculated based on a time bandwidth product. Their corresponding FWHM transform-limited pulse duration is anticipated to be longer than 168 fs, 429 fs, and 334 fs for Ports 1, 2 and 3, respectively. For the power development curve shown in Fig. 4(d)–(f), the

TABLE I
2×2 AND 3×3 NALM LASER CHARACTERISTIC

Laser	2×2 NALM		3×3 NALM
	50:50	70:30	
f (MHz)	/	3.6	3.9
P_P ML initiation (1) (mW)	> 561	299.6	299.6
P_P stable ML (2) (mW)	/	162.6	119.9
P_P ratio of (1) to (2)	/	1.8	2.5
P_{out} (mW)	3.157	2.430	2.189 / 1.896 / 2.754 (6.839 in total)
Δλ (nm)	/	7.00	15.67 / 7.90 / 6.16
τ (fs)	/	> 379	> 168 / 429 / 334

*f = repetition rate, P_P = pump power, P_{out} = output power, Δλ = spectral-bandwidth at FWHM, τ = pulse duration at FWHM.

pump power threshold for continuous-wave laser is measured at 57.46 mW for all ports, which is higher than the 2×2 OC NALM laser cavity. This is because the two laser cavities have different cavity loss and output ratio. All port shows a similar mode-locked (ML) laser output at a pump power threshold of 299.6 mW, while stable ML laser operation is maintained above 119.9 mW. A clear linear dependence on pump power is observed, while the ML laser slope efficiencies of Port-1, 2 and 3 are calculated to be ∼0.98%, ∼0.71% and ∼1.17%, respectively. Furthermore, the maximum pulse energy observed at the highest pump power of 299.6 mW is deduced to be ∼0.56 nJ, ∼0.49 nJ and ∼0.70 nJ for Port-1, 2 and 3, respectively. Hence, Port-3 shows the highest output power, slope efficiency and pulse energy, followed by Port-1 and Port-2.

We compare the laser characteristics between 2×2 OC and 3×3 OC NALM laser cavities in Table I. For the symmetrical 2×2 OC NALM laser cavity, the pump power threshold for initiation of mode-locking is higher than 561 mW. For the asymmetrical 2×2 OC NALM laser cavity with splitting ratio of 70:30, the initiation of mode-locking is obtained at 299.6 mW, while stable mode-locking operation is maintained when the pump power is reduced to 162.6 mW. The pump power threshold required by the 3×3 OC NALM laser cavity to initiate mode-locking (299.6 mW) is reduced by at least 45% as compared with that of the symmetrical 2×2 OC NALM laser cavity (> 561 mW). A pump power as low as 119.9 mW can still maintain stable mode-locking operation, which is 26% lower than that in the asymmetrical 2×2 OC NALM laser cavity. This result demonstrates that the 120-degree phase difference of the 3×3 OC significantly improves mode-locking initiation and stabilization capability. Additionally, at the pump power of 299.6 mW, the total output power of the 3×3 OC NALM laser cavity is 6.839 mW, which is at least two times higher than that of the 2×2 OC NALM laser cavity.

IV. Conclusion

We have fabricated a low-threshold bismuth-doped mode-locked NALM fiber laser operating at 1310 nm, by using a 3×3 OC. Based on the ∼40 meters bismuth-doped phosphosilicate gain fiber laser, stable mode-locking pulse is achieved with a SNR of ∼60 dB, a repetition rate of ∼3.9 MHz and a slope

efficiency of ∼1.17%. The center wavelength and mode-locking threshold remained stabilized at ∼1340 nm and 119.9 mW, respectively. We carried out a comparative analysis between the 2×2 and the 3×3 NALM configurations and the results highlight the superior mode-locking capabilities of the latter. In particular, the pump power threshold for initiation of mode-locking is higher than 561 mW for the symmetrical 2×2 OC NALM laser cavity. Furthermore, the initiation of mode-locking laser is measured at a pump power threshold of 299.6 mW for the asymmetrical 2×2 OC NALM laser cavity with splitting ratio of 70:30, while stable mode-locked laser operation is maintained above 162.6 mW. In comparison to the symmetrical 2×2 OC NALM, owing to the 120-degree phase difference offered by the symmetric 3×3 OC, the mode-locking initiation threshold of the 3×3 NALM is significantly reduced by 45% to 299.6 mW. Moreover, stable mode-locked laser operation is maintained above 119.9 mW, which is 26% lower than that in asymmetrical 2×2 OC NALM laser cavity. Furthermore, the total output power and pulse energy of the 3×3 NALM is measured to be 6.839 mW and 1.75 nJ, representing at least a twofold increase over the 2×2 NALM. This result demonstrates the efficacy of utilizing a 3×3 OC to enhance mode-locking in the Fo8 laser cavity, offering a promising avenue for improving mode-locking performance without the need for additional modulation mechanisms or long single-mode fibers (SMF-28e).

REFERENCES

[1] D. G. Revin, M. Hemingway, Y. Wang, J. W. Cockburn, and A. Belyanin, "Active mode locking of quantum cascade lasers in an external ring cavity," *Nature Commun.*, vol. 7, May 2016, Art. no. 11440.

[2] G. Herink, B. Jalali, C. Ropers, and D. R. Solli, "Resolving the build-up of femtosecond mode-locking with single-shot spectroscopy at 90 MHz frame rate," *Nature Photon.*, vol. 10, pp. 321–326, Mar. 2016.

[3] K. Yin, B. Zhang, J. M. Yao, L. Y. Yang, S. P. Chen, and J. Hou, "Highly stable, monolithic, single-mode mid-infrared supercontinuum source based on low-loss fusion spliced silica and fluoride fibers," *Opt. Lett*, vol. 41, no. 5, pp. 946–949, Mar. 2016.

[4] A. B. Fedotov et al., "Laser micromachining of microstructure fibers with femtosecond pulses," *Laser Phys*, vol. 13, pp. 657–663, Apr. 2003.

[5] Y. Zaouter, F. Guichard, C. Hoenninger, E. Mottay, M. Hanna, and P. Georges, "High average power 600 μj ultrafast fiber laser for micromachining application," *J. Laser Appl.*, vol. 27, Feb. 2015, Art. no. S2.

[6] L. H. Lei et al., "Miniature fabry-perot cavity based on Fiber bragg gratings fabricated by Fs laser micromachining technique," *Nanomaterials*, vol. 11, no. 10, Sep. 2021, Art. no. 2505.

[7] V. V. Tuchin, "Lasers and Fiber optics in biomedicine," *Laser Phys.*, vol. 3, Jun. 1993, Art. no. 767.

[8] D. J. Richardson, R. I. Laming, D. N. Payne, M. W. Phillips, and V. J. Matsas, "320 fs soliton generation with passively mode-locked erbium fiber laser," *Electron. Lett.*, vol. 27, no. 9, pp. 730–732, Apr. 1991.

[9] V. V. Dvoirin, V. M. Mashinsky, O. I. Medvedkov, A. A. Umnikov, A. N. Gur'yanov, and E. M. Dianov, "Bismuth-doped telecommunication fibres for lasers and amplifiers in the 1400-1500-nm region," *Quantum Electron.*, vol. 39, no. 6, Mar. 2009, Art. no. 583.

[10] M. Hofer, M. E. Fermann, F. Haberl, and J. E. Townsend, "Active mode locking of a neodymium-doped fiber laser using intracavity pulse compression," *Opt. Lett.*, vol. 15, no. 24, pp. 1467–1469, Dec. 1990.

[11] J. N. Maran, S. LaRochelle, and P. Besnard, "Erbium-doped fiber laser simultaneously mode locked on more than 24 wavelengths at room temperature," *Opt. Lett.*, vol. 28, no. 21, pp. 2082–2084, Nov. 2003.

[12] M. Tang, X. L. Tian, P. Shum, S. N. Fu, H. Dong, and Y. D. Gong, "Four-wave mixing assisted self-stable 4x10 GHz actively mode-locked erbium fiber ring laser," *Opt. Exp.*, vol. 14, no. 5, pp. 1726–1730, Mar. 2006.

[13] G. Yao, Z. G. Zhao, Z. J. Liu, X. B. Gao, and Z. H. Cong, "High repetition rate actively mode-locked Er: Fiber laser with tunable pulse duration," *Chin. Opt. Lett.*, vol. 20, no. 7, May 2022, Art. no. 071402.

[14] F. Krausz, T. Brabec, and C. Spielmann, "Self-starting passive mode-locking," *Opt. Lett.*, vol. 16, no. 4, pp. 235–237, Feb. 1991.

[15] M. Y. Zhang, H. Chen, J. D. Yin, J. T. Wang, J. Z. Wang, and P. G. Yan, "Recent development of saturable absorbers for ultrafast lasers," *Chin. Opt. Lett.*, vol. 19, no. 8, Aug. 2021, Art. no. 081405.

[16] U. Keller et al., "Semiconductor saturable absorber mirrors (SESAM's) for femtosecond to nanosecond pulse generation in solid-state lasers," *IEEE J. Sel. Topics Quantum Electron.*, vol. 2, no. 3, pp. 435–453, Sep. 1996.

[17] F. Wang et al., "Wideband-tuneable, nanotube mode-locked, fibre laser," *Nature Nanotechnol.*, vol. 3, pp. 738–742, Nov. 2008.

[18] A. Khegai et al., "Bismuth-doped fiber laser at 1.32 μm mode-locked by single-walled carbon nanotubes," *Opt. Exp.*, vol. 26, no. 18, pp. 23911–23917, Sep. 2018.

[19] M. Z. E. Rafique, A. Basiri, J. Bai, J. W. Zuo, and Y. Yao, "Ultrafast graphene-plasmonic hybrid metasurface saturable absorber with low saturation fluence," *ACS Nano*, vol. 17, no. 11, pp. 10431–10441, May 2023.

[20] Q. L. Bao et al., "Atomic-layer graphene as a saturable absorber for ultrafast pulsed lasers," *Adv. Funct. Mater.*, vol. 19, pp. 3077–3083, Oct. 2009.

[21] S. Y. Ryu, K. S. Kim, J. Kim, and S. Kim, "Degradation of optical properties of a film-type single-wall carbon nanotubes saturable absorber (SWNT-SA) with an Er-doped all-fiber laser," *Opt. Exp.*, vol. 20, no. 12, pp. 12966–12974, May 2012.

[22] O. G. Gu et al., "Generation of 131 fs mode-locked pulses from 2.8 μm Er:ZBLAN fiber laser," *Chin. Opt. Lett.*, vol. 18, no. 3, Mar. 2020, Art. no. 031402.

[23] N. J. Doran and D. Wood, "Nonlinear optical loop mirror," *Opt. Lett.*, vol. 13, no. 1, pp. 56–58, Jan. 1988.

[24] T. Noronen, O. Okhotnikov, and R. Gumenyuk, "Electronically tunable thulium-holmium mode-locked fiber laser for the 1700-1800 nm wavelength band," *Opt. Exp.*, vol. 24, no. 13, pp. 14703–14708, Jun. 2016.

[25] J. Zou, C. Dong, H. Wang, T. Du, and Z. Luo, "Towards visible-wavelength passively mode-locked lasers in all-fibre format," *Light Sci. Appl.*, vol. 9, Apr. 2020, Art. no. 61.

[26] D. C. Kirsch, S. Chen, R. Sidharthan, Y. Chen, S. Yoo, and M. Chernysheva, "Short-wave IR ultrafast fiber laser systems: Current challenges and prospective applications," *J. Appl. Phys.*, vol. 128, no. 18, Nov. 2020, Art. no. 180906.

[27] Y. Li et al., "Wavelength-tunable dissipative soliton from Yb-doped fiber laser with nonlinear amplifying loop mirror," *Chin. Opt. Lett.*, vol. 21, no. 6, Jun. 2023, Art. no. 061402.

[28] J. Q. Zhou and J. J. Gu, "32-nJ 615-fs stable dissipative soliton ring cavity Fiber laser with Raman scattering," *IEEE Photon. Technol. Lett.*, vol. 28, no. 4, pp. 453–456, Feb. 2016.

[29] J. W. Nicholson and M. Andrejco, "A polarization maintaining, dispersion managed, femtosecond figure-eight fiber laser," *Opt. Exp.*, vol. 14, no. 18, pp. 8160–8167, Sep. 2006.

[30] R. G. Priest, "Analysis of Fiber interferometer utilizing 3 x 3 Fiber coupler," *IEEE Trans. Microw. Theory Tech.*, vol. TMTT-30, no. 10, pp. 1589–1591, Oct. 1982.

[31] D. Kim, D. Kwon, B. Lee, and J. Kim, "Polarization-maintaining nonlinear-amplifying loop-mirror mode-locked fiber laser based on a 3 × 3 coupler," *Opt. Lett.*, vol. 44, no. 5, pp. 1068–1071, Mar. 2019.

[32] D. Cairns, J. McCowat, N. Langford, and G. E. Town, "Mode-locked operation of a figure-of-eight erbium-doped fiber laser based on a 3x3 non-linear loop mirror," in Proc. *Tech. Dig. Summaries Papers Presented Conf. Lasers Electro-Opt. Postconf. Tech. Dig.*, 2001, pp. 298–299.

[33] M. Pielach, A. Jamrozik, K. Krupa, and Y. Stepanenko, "Self-starting mode-locking in an all-PM Yb-doped fiber laser oscillator enabled by a 3×3 nonlinear optical lossy loop mirror," *Opt. Exp.*, vol. 31, no. 25, pp. 42136–42149, Dec. 2023.

[34] F. Graf, R. Scelle, H. Diekamp, A. Budnicki, and T. Dekorsy, "Femtosecond fiber oscillator based on a 3 × 3-coupler-NALM: Numerical model and realizations at 1 and 2 µm," *Opt. Exp.*, vol. 30, no. 8, pp. 12555–12564, Apr. 2022.

[35] S. K. Sheem, "Optical fiber interferometers with [3 × 3] directional couplers: Analysis," *J. Appl. Phys.*, vol. 52, no. 6, pp. 3865–3872, Jun. 1981.

[36] K. Smith, N. J. Doran, and P. G. J. Wigley, "Pulse shaping, compression, and pedestal suppression employing a nonlinear-optical loop mirror," *Opt. Lett.*, vol. 15, no. 22, pp. 1294–1296, Nov. 1990.

[37] J. Zhao et al., "Nonlinear absorbing-loop mirror in a holmium-doped fiber laser," *J. Light. Technol.*, vol. 38, no. 21, pp. 6069–6075, Nov. 2020.

[38] N. Seong, D. Y. Kim, and S. P. Veetil, "Mode-locked fiber laser based on an attenuation-imbalanced nonlinear optical loop mirror," *Opt. Commun.*, vol. 280, no. 2, pp. 438–442, Dec. 2007.

[39] W. Wang, F. Wang, Y. Zhang, H. Ma, Q. Yu, and X. Zhang, "Passively mode-locked figure-eight fiber laser using a compact power-imbalanced nonlinear optical-loop mirror," *J. Russain Laser Res.*, vol. 37, no. 3, pp. 265–272, Jul. 2016.

[40] J. Shi et al., "All-polarization-maintaining figure-eight Er-fiber ultrafast laser with a bidirectional output coupler in the loss-imbalanced nonlinear optical loop mirror," *Chin. Opt. Lett.*, vol. 16, no. 12, Nov. 2018, Art. no. 121404.

[41] S. K. Wang, Q. Y. Ning, A. P. Luo, Z. B. Lin, Z. C. Luo, and W. C. Xu, "Dissipative soliton resonance in a passively mode-locked figure-eight fiber laser," *Opt. Exp.*, vol. 21, no. 2, pp. 2402–2407, Jan. 2013.

[42] A. Khegai et al., "The influence of the MCVD process parameters on the optical properties of bismuth-doped phosphosilicate fibers," *J. Lightw. Technol.*, vol. 38, no. 21, pp. 6114–6120, Nov. 2020.

[43] K. Y. Lau, S. Firstov, Y. D. Cui, X. F. Liu, F. Afanasiev, and J. R. Qiu, "Highly efficient O-band rectangular pulse emission in a figure-of-nine bismuth-doped fiber laser," *J. Light. Technol.*, vol. 41, no. 19, pp. 6383–6388, Oct. 2023.

[44] E. M. Dianov, S. V. Firstov, V. F. Khopin, A. N. Guryanov, and I. A. Bufetov, "Bi-doped fibre lasers and amplifiers emitting in a spectral region of 1.3 μm," *Quantum Electron.*, vol. 38, no. 7, pp. 615–617, Jul. 2008.

[45] E. M. Dianov, "Bismuth-doped optical fibers: A challenging active medium for near-IR lasers and optical amplifiers," *Light Sci. Appl.*, vol. 1, May 2012, Art. no. e12.